

UC Irvine

UC Irvine Previously Published Works

Title

Power-dependent speciation of volatile organic compounds in aircraft exhaust

Permalink

<https://escholarship.org/uc/item/5mc232m9>

Authors

Beyersdorf, AJ
Thornhill, KL
Winstead, EL
[et al.](#)

Publication Date

2012-12-01

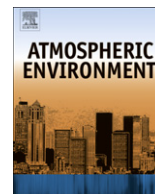
DOI

10.1016/j.atmosenv.2012.07.027

Copyright Information

This work is made available under the terms of a Creative Commons Attribution License, available at <https://creativecommons.org/licenses/by/4.0/>

Peer reviewed



Power-dependent speciation of volatile organic compounds in aircraft exhaust

Andreas J. Beyersdorf^{a,*}, K. Lee Thornhill^{a,b}, Edward L. Winstead^{a,b}, Luke D. Ziemba^a, Donald R. Blake^c, Michael T. Timko^d, Bruce E. Anderson^a

^a NASA Langley Research Center, Hampton, VA 23662, USA

^b Science Systems and Applications, Inc., Hampton, VA 23666, USA

^c University of California Irvine, Irvine, CA 92697, USA

^d Aerodyne Research, Inc., Billerica, MA 01821, USA

H I G H L I G H T S

- ▶ At low power, scaling hydrocarbons to ethene reduces variability amongst engines.
- ▶ At high power, there is a difference in composition with aromatics dominating.
- ▶ At low power, thermal cracking dominates.
- ▶ At high power, aromatic species are formed via the HACA process in the exhaust.
- ▶ In downwind samples, HAPs make up a large portion of measured emissions (27–42%).

A R T I C L E I N F O

Article history:

Received 28 March 2012

Received in revised form

15 June 2012

Accepted 12 July 2012

Keywords:

Aircraft emissions

Turbine engine

Hydrocarbon emission indices

Oxygenated hydrocarbons

A B S T R A C T

As part of the third NASA Aircraft Particle Emissions Experiment (APEX-3, November 2005), whole air samples were collected to determine the emission rates of volatile organic compounds (VOCs) from aircraft equipped with three different gas-turbine engines (an Allison Engine 3007-A1E, a Pratt–Whitney 4158, and a Rolls–Royce RB211-535E4B). Samples were collected 1 m behind the engine exhaust plane of the engines while they were operated at powers ranging from idle up to 30% of maximum rated thrust.

Exhaust emission indices (mass emitted per kilogram of fuel used) for CO and non-methane hydrocarbons (NMHCs) were calculated based on enhancements over background relative to CO₂. Emissions of all NMHCs were greatest at low power with values decreasing by an order of magnitude with increasing power. Previous studies have shown that scaling idle hydrocarbon emissions to formaldehyde or ethene (which are typically emitted at a ratio of 1-to-1 at idle) reduces variability amongst engine types. NMHC emissions were found to scale at low power, with alkenes contributing over 50% of measured NMHCs. However, as the power increases hydrocarbon emissions no longer scale to ethene, as the aromatics become the dominant species emitted. This may be due in part to a shift in combustion processes from thermal cracking (producing predominantly alkenes) to production of new molecules (producing proportionally more aromatics) as power increases. The formation of these aromatics is an intermediate step in the production of soot, which also increases with increasing power. The increase in aromatics relative to alkenes additionally results in a decrease in the hydroxyl radical reactivity and ozone formation potential of aircraft exhaust.

Samples collected 30 m downwind of the engine were also analyzed for NMHCs and carbonyl compounds (acetone, 2-butanone and C₁–C₉ aldehydes). Formaldehyde was the predominant carbonyl emitted; however, the ratio of ethene-to-formaldehyde varied between the aircraft, possibly due to the sampling of transient emissions such as engine start-up and power changes. A large portion of the measured emissions (27–42% by mass) in the plume samples was made up of hazardous air pollutants (HAPs) with oxygenated compounds being most significant.

Published by Elsevier Ltd.

1. Introduction

The emission of volatile organic compounds (VOCs) into the atmosphere adversely affects the environment including production of ozone and increased levels of greenhouse gases and

* Corresponding author. Tel.: +1 757 864 8264; fax: +1 757 864 6326.

E-mail address: andreas.j.beyersdorf@nasa.gov (A.J. Beyersdorf).

hazardous air pollutants (HAPs). The primary anthropogenic source of VOC emissions is the combustion of fossil fuels and related evaporation. Aircraft usage is a minor consumer of fossil fuels, accounting for only 3% of total usage. However, total jet fuel usage in the United States is projected to increase by 130% between 2009 and 2030 (Federal Aviation Agency (FAA), 2010). In addition, aircraft emissions are unique in that they directly affect the atmosphere both at ground level (aircraft taxi, idling, take-off and landing) and at cruise altitudes (upper troposphere and lower stratosphere).

The complete combustion of jet fuel results in the formation of carbon dioxide (CO₂) as the only carbonaceous species. However, because of combustion inefficiencies, other carbon-containing compounds are emitted both as gaseous and particulate species. To quantify the impact of these emissions, the International Civil Aviation Organization (ICAO) requires manufacturers to measure and document carbon monoxide (CO), unburned hydrocarbons, and smoke number emissions from all engines used in civil aircraft at power settings equivalent to idle (7% of rated thrust), airport approach (30%), climb-out (85%) and take-off (100%). While these “certification tests” yield estimates of total carbonaceous species emissions, they provide no information on hydrocarbon speciation and thus no insight into the reactivity or hazardous nature of the exhaust.

A number of investigations have studied the speciation of emitted non-methane hydrocarbons (NMHCs). These include measuring the exhaust directly behind the aircraft engines while on the ground (Spicer et al., 1992, 1994; Anderson et al., 2006; Knighton et al., 2007; Yelvington et al., 2007; Timko et al., 2010a), behind an in-flight aircraft (Slemr et al., 1998, 2001), and in wind-advected aircraft exhaust plumes at airports (Herndon et al., 2006, 2009; Schürmann et al., 2007).

The sum of NMHCs in aircraft exhaust is highly dependent on engine power with the highest emission at power settings typical of ground idle and decreasing as power increases. The organic fraction of the exhaust is composed primarily of short-chain unsaturated hydrocarbons (Anderson et al., 2006) and aldehydes (Spicer et al., 1994). In particular, the predominant species emitted are ethene and formaldehyde (HCHO) at a ratio of 1:1 (Herndon et al., 2009). This is in strong contrast to the composition of unburned jet fuel which is composed primarily of C₁₁–C₁₄ hydrocarbons (Spicer et al., 1994). The short-chained species found in the exhaust are produced from fuel cracking (alkenes) and partial oxidation (forming formaldehyde) during combustion (Warnatz et al., 2006). In a recent study looking at exhaust plumes from multiple aircraft while on an active runway, Herndon et al. (2009) showed that scaling the near-idle power emission indices (EIs) to tracers of fuel cracking (formaldehyde or ethene) eliminated much of the variability between engine types. However, some evidence points to variation in the hydrocarbon speciation profile with changes in engine power setting, with higher engine power settings producing a larger fraction of aromatics and alkanes (Anderson et al., 2006). The formation of aromatics is an intermediate step in the formation of

soot (Warnatz et al., 2006) which also increases as aircraft engine power increases. The soot formation process proceeds via hydrogen abstraction/carbon addition (HACA) which first forms aromatic species, then polycyclic aromatic hydrocarbons (PAHs), and finally soot (Bauer and Jeffers, 1988; Wang and Frenklach, 1994; McEnally and Pfefferle, 1997).

The power-dependent speciation of emitted VOCs was a focus of the third Aircraft Particle Emission Experiment (APEX-3) at the NASA Glenn Research Center in Cleveland, Ohio during November 2005 (Wey et al., 2006). This project focused on the quantification and speciation of both particulate and gaseous emissions from different engines. Results from the particulate sampling are given in Timko et al. (2010b) and Kinsey et al. (2011), while gas-phase measurements of nitrogen oxides and formaldehyde are found in Timko et al. (2010a). The current analysis reports emissions of NMHCs directly behind the aircraft engine (non-oxygenated species only) and in exhaust plumes downwind from the engines (including carbonyls).

2. Sample collection

During APEX-3, aircraft were parked and chocked on a side portion of the tarmac at Cleveland Hopkins International Airport in Cleveland, Ohio. The thrust of the engines was then varied from conditions typical of idle (4% of full rated thrust) to take-off (93%). Samples were collected using an inlet probe positioned one meter behind the engine exit plane. The sample was immediately diluted with dry nitrogen, resulting in a variable dilution ratio between 4:1 and 90:1. Dry nitrogen dilution was necessary for concurrent aerosol measurement (dilution reduces aerosol processing in the sampling lines and allows for aerosol concentrations within the detection limits of the instruments; Wong et al., 2011). A pump drew the exhaust through stainless steel tubing to a mobile lab where samples were collected in two-liter stainless steel canisters. In total, 20 direct exhaust samples were collected from three engine types at powers between 4 and 30% (Table 1).

Plume samples were collected by the U.S. Environmental Protection Agency's (EPA's) National Risk Management Research Laboratory using its Diesel Emissions Aerosol Laboratory (Kinsey et al., 2006). The EPA extracted a continuous sample from the engine exhaust plume 30 m behind the exit plane. To obtain sufficient sample for analysis, time-integrated sampling of the plumes was performed for each engine encompassing multiple engine thrust settings as described by Kinsey (2009). Samples were collected for analysis of NMHCs (in evacuated stainless steel canisters) and carbonyls (using 2,4-dinitrophenylhydrazine [DNPH] impregnated silica gel cartridges equipped with potassium iodide ozone scrubbers). During transport and in the field, the silica gel cartridges were stored at approximately –20 °C. Background mixing ratios were also sampled by an independent sample extraction and analysis system. Additional details on the EPA sampling campaign are provided in the final EPA report for the three APEX campaigns (Kinsey, 2009).

Table 1
AAFEX test parameters and number of samples collected.

Aircraft & Engine Properties		Fuel Properties		Number of Samples Collected		
Aircraft	Engine Type	Sulfur (ppm)	Aromatics (%)	Direct Exhaust		Plume
				4–8%	15–30%	
Embraer ERJ 145 ^a	Allison Engine 3007-A1E (AE3007)	300	20.7	6	2	2
Airbus A300	Pratt–Whitney 4158 (PW4158)	600	16.2	2	2	2
Boeing 757 ^b	Rolls–Royce RB211-535E4B (RB211)	300	20.3	6	2	1

^a Samples collected behind the right and left engines of the same aircraft.

^b Two Boeing 757s with RB211 engines were sampled for the direct exhaust and one for the downwind sample.

3. Sample analysis

After the experiment, the direct exhaust samples were analyzed at the University of California, Irvine (UCI) using gas chromatography for the measurement of CO₂, NMHCs and halogenated hydrocarbons. However, only CO₂ and NMHC data are presented here because emission rates of halocarbon species were found to be small. Carbon dioxide was separated by GC and quantified by a thermal conductivity detector. Non-methane hydrocarbons and halocarbons were measured using a three GC system featuring a quadrupole mass selective detector (MSD), two electron capture detectors (ECDs) and three flame ionization detectors (FIDs; Colman et al., 2001). In brief, an aliquot of each sample was pre-concentrated in a stainless steel loop containing glass beads cooled with liquid nitrogen. The loop was heated to re-volatilize the

sample, which was then flushed by a helium carrier, split into six streams, and output to different column–detector combinations. The NMHCs were detected using the FIDs and the MSD. Quantification of the compounds was performed by the analysis of whole air standards after every eight samples. The limit of detection (LOD) was 3 pptv for all compounds. Samples were pressurized and analyzed within a month after collection, both factors which have been shown to increase sample integrity (Apel et al., 2003).

Analysis of the 30-m downwind VOC canister samples was performed using similar GC-MSD and GC-FID systems. The approach is a combination of EPA Methods TO-15 (EPA, 1999a) and CB-4 (EPA, 1986), used to resolve air toxics and hydrocarbon species. Carbonyl samples collected on the DNPH silica gel cartridges were extracted and analyzed using a High Pressure Liquid Chromatograph (HPLC) equipped with an ultraviolet (UV)

Table 2
Emission indices (mg kg^{−1} of fuel) for VOCs measured in the direct exhaust samples.

Engine	AE3007			PW4158			RB211		
Power	8% ^e	15%	30%	7% ^e	15%	30%	4% ^e	7%	15%
Samples Collected	6	1	1	2	1	1	4	2	2
CO	21,000 ± 5000	11,000	3600	36,000 ± 12,000	6700	3000	59,000 ± 32,000	5900	3700
Ethane	27 ± 4	15	7.2	48 ± 11	8.2	1.5	16 ± 7	10	6.9
Propane	14 ± 3	12	4.5	8.2 ± 2.7	5.7	1.1	8.3 ± 3.6	6.5	4.2
n-Butane	7.8 ± 2.2	6.1	3.6	2.4 ± 1.8	6.9	1.1	5.1 ± 2.6	4.5	3.1
i-Butane	3.2 ± 0.9	2.8	1.5	1.1 ± 1.0	2.6	0.42	2.1 ± 1.2	1.9	1.4
n-Pentane	2.7 ± 0.8	2.4	1.2	1.8 ± 0.8	2.3	0.39	2.1 ± 0.8	1.7	1.3
i-Pentane	2.9 ± 1.1	2.4	1.1	1.5 ± 0.7	4.5	0.61	2.9 ± 1.3	2.7	1.6
n-Hexane ^d	1.8 ± 1.4	1.2	0.45	3.1 ± 0.3	1.7	0.23	1.3 ± 0.5	1.1	0.80
2-Methylpentane	1.0 ± 0.7	0.32		1.6 ± 0.1	0.35	0.27	0.94 ± 0.64	1.1	0.37
3-Methylpentane	0.76 ± 0.72	0.34	0.17	1.0 ± 0.4	0.89	0.08	0.47 ± 0.26	0.38	0.23
n-Heptane	0.71 ± 0.22	0.57	0.20	1.2 ± 0.2	0.46	0.08	0.43 ± 0.19	0.33	0.19
n-Octane	0.74 ± 0.24	0.60	0.15	1.08 ± 0.04	1.0	0.20	0.42 ± 0.15	0.26	0.22
Ethene	316 ± 122	50	2.6	668 ± 7	37	0.76	112 ± 72	16	2.9
Propene	85 ± 34	8.9	3.2	350 ± 112	8.5	0.21	32 ± 19	3.6	0.79
1-Butene	19 ± 8	1.7	0.10	92 ± 28	1.9	0.12	7.7 ± 4.2	0.86	0.29
i-Butene	7.2 ± 2.9	1.0	0.21	35 ± 7	1.1	0.49	3.4 ± 1.7	0.59	0.68
cis-2-Butene	1.5 ± 0.7	0.06		8.2 ± 2.8	0.22	0.03	0.63 ± 0.34	0.07	0.03
trans-2-Butene	2.4 ± 1.0	0.20	0.02	12 ± 3	0.32	0.02	0.98 ± 0.51	0.15	0.07
1,3-Butadiene	11 ± 3	0.61	3.7	94 ± 15	2.5	0.48	6.2 ± 3.1	0.54	0.09
1-Pentene	7.3 ± 2.8	0.18		39 ± 12	0.83	0.13	3.2 ± 1.7	0.82	0.05
cis-2-Pentene	0.54 ± 0.23			3.2 ± 0.9	0.10	0.01	0.24 ± 0.14	0.08	0.01
trans-2-Pentene	0.90 ± 0.41	0.02	0.02	5.1 ± 1.5	0.18	0.02	0.38 ± 0.21	0.06	0.05
2-Methyl-1-Butene	1.9 ± 0.8	0.10		11 ± 3	0.30	0.03	0.90 ± 0.31	0.10	0.06
2-Methyl-2-Butene	2.4 ± 0.7	0.57	0.21	13 ± 3	0.61	0.07	1.2 ± 0.4	0.45	0.30
3-Methyl-1-Butene	1.9 ± 0.8	0.17	0.17	11 ± 4	0.21	0.02	0.81 ± 0.44	0.13	0.06
Ethyne	201 ± 79	38	2.4	264 ± 94	17	0.49	69 ± 43	10	2.2
Propyne	1.1 ± 0.4	0.08		5.3 ± 1.5	0.11	0.01	0.43 ± 0.21	0.05	0.03
Benzene	65 ± 23	12	3.4	147 ± 47	10	0.91	24 ± 14	6.0	4.1
Toluene	29 ± 9	8.9	3.8	101 ± 31	12	2.8	15 ± 6	7.9	5.8
Ethylbenzene	3.4 ± 1.2	0.72	0.52	17 ± 5	2.7	0.42	1.7 ± 0.7	0.85	0.64
Styrene	6.1 ± 1.3	0.55	0.97	12 ± 10	4.0	0.15	4.9 ± 1.6	4.9	2.3
o-Xylene	3.7 ± 1.3	0.8	0.91	23 ± 7	3.7	0.82	2.0 ± 0.9	1.2	0.91
m-Xylene	5.4 ± 1.5	1.6	1.2	41 ± 12	6.7	1.3	3.1 ± 1.2	1.9	1.4
p-Xylene	1.5 ± 0.7	0.51	0.16	8.7 ± 3.0	1.8	0.36	0.86 ± 0.24	0.58	0.55
n-Propylbenzene	1.1 ± 0.5	0.33	0.36	6.3 ± 1.4	0.92	0.80	0.83 ± 0.50	0.91	0.27
i-Propylbenzene	0.43 ± 0.24	1.00	0.06	3.2 ± 0.9	0.29	0.10	0.24 ± 0.09	0.15	0.20
Trimethylbenzene ^a	9.1 ± 4.6	3.4	4.8	46 ± 8	9.5	6.6	6.2 ± 3.2	6.8	2.9
Ethyltoluene ^a	5.0 ± 2.4	1.7	2.1	27 ± 7	4.4	4.7	3.9 ± 2.8	4.7	1.5
Total NMHC	851	176	51	2113	161	28	341	100	48
ICAO ^b	3520		30	1780		140		140	
Formaldehyde ^c	530		6	1010			150		
Ethene/Formaldehyde	0.60		0.43	0.66			0.75		
Total HAPs	127	27	15.10	446.90	45	7	58.50	25	16.61
Fraction of Emissions ^d	0.15	0.15	0.30	0.21	0.28	0.27	0.17	0.25	0.34

^a 3 isomers of trimethylbenzene and 3 isomers of ethyltoluene.

^b ICAO emission indices for total unburned hydrocarbons (includes oxygenates).

^c From Timko et al. (2010a); AE3007 and RB211 values are averages of two engines.

^d Shaded compounds are classified as HAPs; Fraction = Total HAPs/Total NMHCs.

^e Uncertainties for the lowest power are the 1 sigma standard deviation.

detector. Sample analysis was performed using a modification of EPA Method TO-11A (EPA, 1999b) to incorporate additional compounds.

4. Data analysis procedures

The dilution factors for the direct exhaust samples were determined by measuring CO₂ in the raw exhaust (by non-dispersive infrared gas analyzers) and in the diluted samples (by the GC system described above). The background mixing ratio of each compound was subtracted from the dilution-corrected mixing ratio to determine the enhancement in compound X measured in the exhaust (ΔX). Background measurements for the VOCs were made by the EPA during periods with no aircraft activity.

The enhancement in the exhaust was then used to determine the emission indices (EIs) for the individual NMHC species. This was accomplished by ratioing the enhancement of a compound to the enhancement in CO₂, which is the most abundant species emitted by aircraft engines and has an emission index of 3160 g CO₂ kg⁻¹ fuel based on complete combustion of the JP-8 fuel used in the tests (Knighton et al., 2007). Using this value, the EI for a compound (EI_X) can be found by

$$EI_X = (\Delta X / \Delta CO_2) \times (M_X / M_{CO_2}) \times (3160 \text{ g CO}_2 \text{ kg}^{-1} \text{ fuel})$$

where ΔX and ΔCO_2 must be in the same units (pptv or ppbv), and M_X and M_{CO_2} are the molar masses (g mol⁻¹) of compound X and CO₂, respectively. Enhancements were deemed significant if they were greater than 100 pptv which is larger than the expected variations in background mixing ratios during the tests. At typical ΔCO_2 values measured (2500–20,000 ppmv), this corresponds to EIs of approximately 100 mg ethene kg⁻¹ fuel and 30 mg benzene kg⁻¹ fuel. Because exhaust mixing ratios are much larger than background values, background variation is believed to be a minor cause of uncertainty. Instead, uncertainties in EIs are dominated by uncertainties in the dilution factor which can be attributed to variations in sample flow and pressure during sample collection. These uncertainties are estimated to be on the order of 20% (Anderson et al., 2006). Emission indices vary with ambient temperature and pressure and were corrected to 15 °C and 1 atm according to the Boeing fuel flow methodology (DuBois and Paynter, 2006). This correction was less than 1.5% for all samples but was performed to facilitate comparison with other experiments.

5. Results – direct exhaust samples

Power dependent emission indices for the NMHCs measured in the direct exhaust and ICAO certification values for the AE3007, PW4158 and RB211 engines are given in Table 2. Halogenated compounds had small background enhancements and are therefore not reported. The total measured NMHC is lower than ICAO estimates of unburned hydrocarbons at idle except for PW4158. This is likely due to the fact that the ICAO measurements include oxygenated species not measured in the direct exhaust during APEX-3. The reason why the measured PW4158 NMHCs emissions are greater than the ICAO certification (even though the compounds included in the field measurement should be only a subset of those included in the ICAO measurement) is unclear. However, in addition to this quantitative difference, the speciation profile of the PW4158 was found to differ from the other engines (see discussion below).

Consistent with the ICAO databank, emissions were highest at idle conditions and decreased dramatically with increasing power

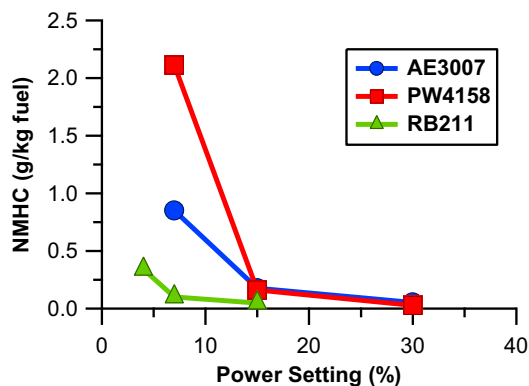


Fig. 1. Total NMHC EIs in the direct exhaust as a function of power for the three engines studied.

(Fig. 1). All engines were tested near 7% (AE3007 at 8%, others at 7%) since it is used as the idle conditions for ICAO certification. However, in practice aircraft are known to idle at lower powers with considerable variability (Herndon et al., 2009). Thus, the RB211 engine exhaust was also sampled at 4% power. Emission indices for the 4% power samples were significantly greater than measured at 7% (a factor of 3.4 for total NMHC and up to an order of magnitude for individual species), suggesting emissions at low power are very sensitive to the actual power setting while at idle. This is also seen in runway studies of idling aircraft (Herndon et al., 2009) and is especially important because of the large amount of time that aircraft spend at idle in comparison to take-off conditions. While fuel flow rates are higher at take-off, the increased EIs seen at idle and longer periods of time at these power conditions cause aircraft idling and taxiing to be the major source of VOC emissions at ground level (similar to calculations made for NO₂ emissions in Wood et al., 2008).

As the power increases, not only do the emission indices decrease but the NMHC speciation changes. At low power, alkenes

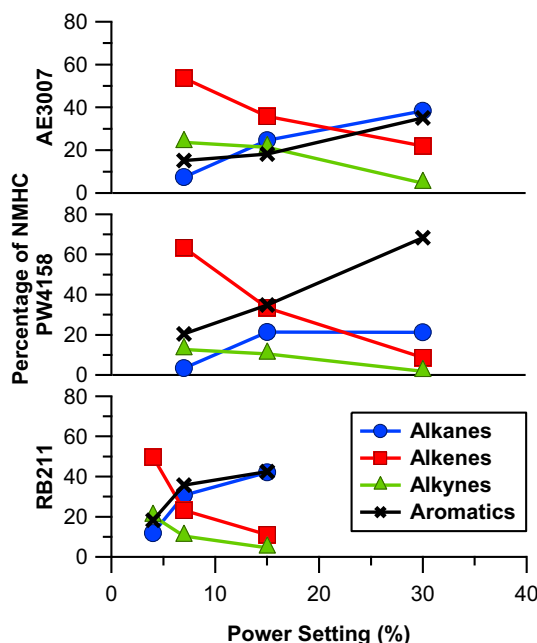


Fig. 2. Alkanes, alkenes, alkynes, and aromatics as a percentage of total NMHCs in the direct exhaust.

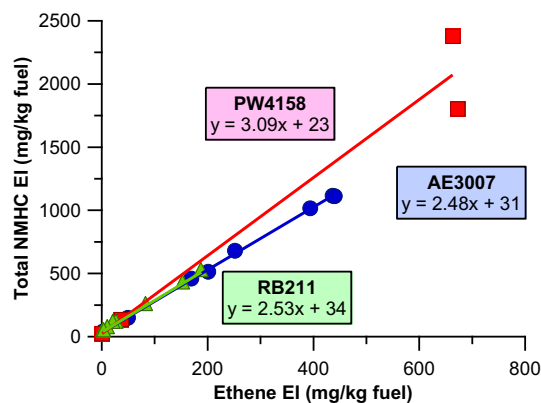


Fig. 3. Total NMHC emission indices for the AE3007 (circles), PW4158 (squares), and RB211 (triangles) engines in the direct exhaust.

are the predominant species accounting for over 50% of the measured NMHC (Fig. 2). However as the power increases, the fractions of alkenes and alkynes both decrease and the fraction of aromatics increases. This suggests a shift in NMHC production processes (discussed below).

In all of the idle samples (4–8% thrust), ethene is the most abundant NMHC measured in the exhaust. A scatter plot of total NMHCs versus ethene shows a good correlation with nearly identical slopes for the AE3007 and RB211 engines (Fig. 3). The PW4158 engine has 18% higher emissions of NMHCs relative to ethene; however these higher values are not significantly different due to the limited sample size at low power (only two PW4158 samples were collected at 7% power). Table 2 also includes formaldehyde data from Timko et al. (2010a) for the same engines measured by a tunable laser differential absorption spectrometer (TILDAS). The ratios of ethene-to-formaldehyde at idle ranged from 0.60 to 0.75 which are lower than previous measurements (0.78–1.26; Herndon et al., 2009). However, these lower than expected ratios could be the result of sampling artifacts from the sampling probe. De la Rosa Blanco et al. (2011) found that hydrocarbons can be oxidized in the probes to form CO. If ethene is preferentially oxidized (or is only partially oxidized to form formaldehyde) the ethene-to-formaldehyde ratio will be lower than in true exhaust.

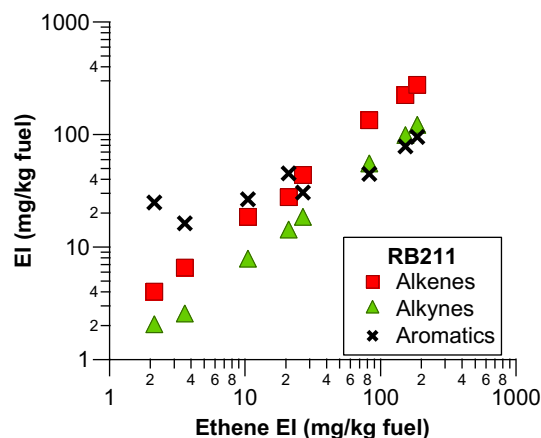


Fig. 4. Emission indices in the direct exhaust for total alkenes, alkynes and aromatics versus ethene EI for the RB211 engines. Logarithmic axes are used to better view the deviation at low emission indices.

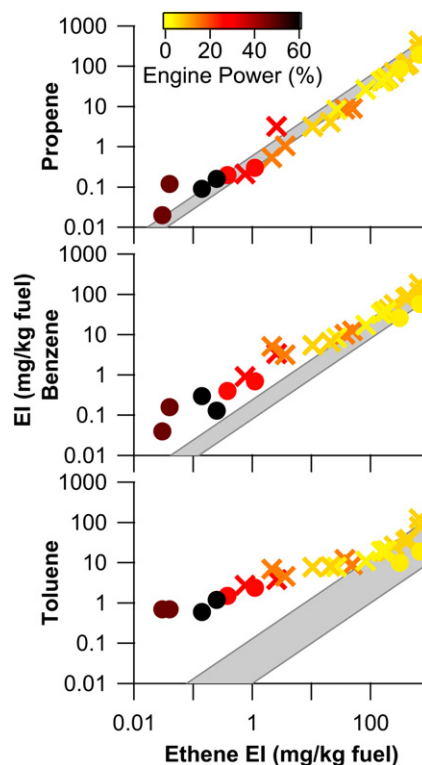


Fig. 5. Emission indices for the RB211 engine (crosses) and EXCAVATE dataset (circles; from Anderson et al., 2006). The data is colored by engine power setting. The shaded area represents the ratios reported by Herndon et al. (2009) at idle conditions. These ratios are for high ethene EIs but have been extended to all ethene values. (For interpretation of the references to colour in this figure legend, the reader is referred to the web version of this article.)

Scaling emissions indices to ethene (as suggested by Herndon et al., 2009) reduced the variability among engines. However, the linear fits can be largely biased by the samples with the highest emission indices (samples collected at low power). The y-intercepts in Fig. 3 are non-zero suggesting a change in the speciation and source with an increase in power (decrease in ethene). Applying the same fitting technique with the different hydrocarbon classes (alkenes, alkynes and aromatics) also gave good correlations (shown for RB211 in Fig. 4). However, the alkenes and alkynes have a near-zero y-intercept while the aromatics have a y-intercept

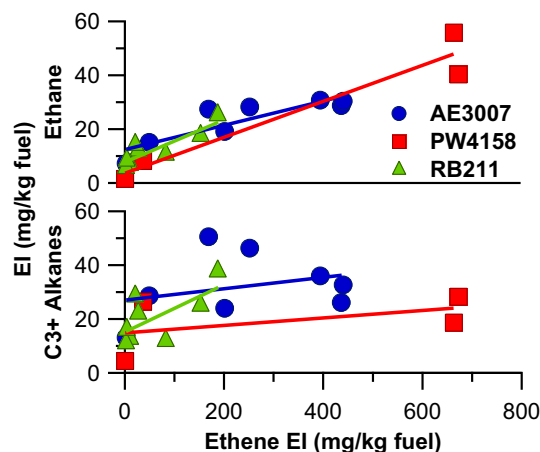


Fig. 6. Emission indices for ethane and larger alkanes versus ethene EI for the three engines tested.

Table 3Emission indices (mg kg⁻¹ of fuel) for VOCs measured in the plume samples.

Engine Type	AE3007	PW4158	RB211
Ethane	33	15	11
Propane	26	0.94	1.1
Butanes	22		
Pentanes	14	0.36	0.54
n-Hexane ^a	2.4		
C _{6–13} Alkanes ^b	16	33	11
Ethene	41	246	194
Propene	9.0	87	62
Butenes		37	25
1,3-Butadiene	1.7	25	18
Pentenenes	20	12	
C _{6–13} Alkenes	3.8	55	71
Ethyne	28	105	128
Benzene	5.5	25	22
Toluene	2.9	10	6.3
C ₂ Benzenes	2.9	16	6.1
C ₃ Benzenes	1.3	25	7.2
C ₄ Benzenes		2.5	1.7
Formaldehyde	117	357	130
Acetaldehyde	70	126	38
Propionaldehyde	7.8	17	6.6
C _{4–9} Aldehydes	4.9	88	34
Acetone	82		
2-Butanone	5.1	4.4	
Glyoxal		112	41
Methylglyoxal		24	10
Alkanes	113	49	23
Alkenes	55	471	382
Alkynes	28	105	128
Aromatics	12.5	78	43
Non-Oxygenated NMHCs	209	703	576
Oxygenated NMHCs	287	729	259
Total HAPs	210	576	228
Fraction of Emissions ^c	0.42	0.40	0.27

^a Shaded compounds are classified as HAPs.^b Other than n-Hexane.^c Total HAPs/(NMHC + Oxygenated).

closer to 20 mg kg⁻¹ fuel. This is also seen in Fig. 5 where propene, benzene and toluene emission indices for the RB211 engine are compared to idle measurements from previous studies (Herndon et al., 2009 and references therein) and measurements during the NASA EXCAVATE campaign (Experiment to Characterize Aircraft Volatile Aerosol and Trace-species Emissions; Anderson et al., 2006). During EXCAVATE, VOC emissions were characterized for a RB211-535-E4 engine (which is an earlier version of the RB211 engine studied during APEX-3) at idle to 61% power. Propene values at all power settings lie along the line defined by the low power data from multiple tests, whereas the aromatics (benzene and

toluene) deviate at high power. The deviation from idle conditions increases as power setting increases (i.e., as the power increases aromatic values show more deviation from the low power data shown in the shaded area). In addition, the benzene-to-toluene ratio changes with power. For the AE3007 engine, the ratio is reduced from 2.2 at low power to 0.9 at high power. The decreasing benzene-to-toluene ratio with increasing power is related to the production of larger, more complex hydrocarbons via the HACA process as power increases.

The correlation of the alkanes with ethene is more difficult to interpret (Fig. 6). The correlation between ethane and ethene is good, but the correlation between larger alkanes and ethene is poor. This suggests that ethane might have a dominant combustion source but the larger alkanes have an additional, non-combustion source such as unburned fuel.

6. Results – EPA plume samples

The samples collected downwind from the aircraft represent a naturally diluted sample of the exhaust. Emission indices were determined using the method described above (Table 3), but the plume samples were collected over a prolonged period encompassing multiple engine powers and thus represent an average emission sample. Time-weighted powers were between 32 and 41%. However, the non-oxygenated NMHC emissions (Fig. 7) were closer to levels measured in the direct exhaust at 7 and 15%. These high values are possibly due to transient emissions such as engine start-up and power changes; Timko et al. (2010b) found that emissions of CO at idle were two times greater at engine start-up than when the engine had already been operated at higher power settings.

The ethene-to-formaldehyde ratio also varied among the samples. This ratio was shown by Herndon et al. (2009) to be fairly stable between 0.76 and 1.26 at idle conditions. Ratios measured in the plumes varied between 0.3 and 1.5. Likewise, Spicer et al. (1994) found a ratio of 0.14 at 80% power for a CFM56 engine (values were near detection limits). This suggests that this ratio is power dependent, most likely due to a shift in combustion processes.

7. Discussion – combustion processes

As mentioned previously, a shift is seen in the NMHC speciation (towards production of aromatics) as engine power increases. This is likely the result of increased engine temperatures and pressures as engine power increases (Wey et al., 2006) causing a shift in combustion processes (Schulz et al., 1999). Fuel cracking is believed to be the primary source of short-chain alkenes and dominates at idle power, while formation of larger compounds (e.g., toluene) can occur at the higher power settings (higher temperatures).

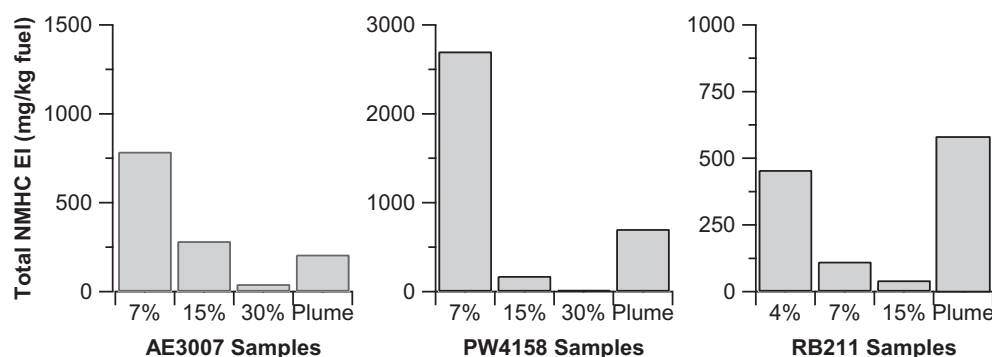


Fig. 7. Total non-oxygenated NMHC emission indices for direct and plumes samples.

Table 4
Fraction of NMHC from cracking and other sources (including pyrolysis).

Power (%)	AE3007		PW4158		RB211	
	Cracking	Other	Cracking	Other	Cracking	Other
7–8	1.00	0.00	1.00	0.00	1.00	0.00
15	0.75	0.25	0.72	0.28	0.39	0.61
30	0.13	0.87	0.08	0.92		

The variance in NMHC emissions with power can be found by examining the NMHC-to-ethene ratio. The ratio at idle (r_{idle} ; using 7–8% power for ease of comparison between engines) gives the amount of emissions expected if the combustion processes are independent of power. If ethene is assumed to be produced strictly via homolytic fission processes associated with fuel cracking, then the amount of NMHC emissions expected from cracking at higher powers is given by:

$$\text{NMHC}_{\text{cracking}} = \text{Ethene}_{\text{high power}} \times r_{\text{idle}}$$

The excess NMHC is therefore presumed to be from other sources:

$$\text{NMHC}_{(\text{other sources})} = \text{NMHC}_{\text{high power}} - \text{NMHC}_{\text{cracking}}$$

Table 4 shows the fraction of NMHC emissions due to fuel cracking as a function of power. At idle, cracking is the only source (by definition), while at higher powers other sources become important (including growth of larger compounds via the HACA process).

This shift in combustion processes with power affects the particulate emissions of the engine. Production of aromatic species via the HACA process can act as an intermediate in the formation of PAHs and soot. However, PAH (Kinsey et al., 2011) and soot (Timko et al., 2010b) emissions follow a 'u'-shaped trend with a decrease in emissions from idle to a minimum at intermediate powers, and then an increase to maximum emissions at 100% power. Thus the formation of PAHs and soot at low power is from aromatics produced by fuel cracking and unburned fuel, while their formation at high power is from aromatics produced via the HACA process.

8. Discussion – ozone formation potential

The shift in hydrocarbon composition as the power changes also affects the reactivity of the exhaust. To analyze this shift, the Maximum Incremental Reactivity (MIR) scale for ozone production is used (Carter, 1994; using updated values from Carter, 2010). The MIR scale relates the amount of ozone (O_3) produced from an incremental increase in the amount of a specific hydrocarbon to the

urban atmosphere. This allows for a scale of ozone production from individual hydrocarbons. As ozone production is highly dependent on the reaction rate of the hydrocarbon with hydroxyl radical, MIR values are also dependent on the hydroxyl reactivity of the hydrocarbon. Therefore, of the compounds measured, alkenes have the highest MIR values (ranging from 6 to 15 $\text{gO}_3/\text{gVOC}^{-1}$) while alkanes ($0.3\text{--}1.8 \text{ gO}_3/\text{gVOC}^{-1}$) and CO ($0.06 \text{ gO}_3/\text{gVOC}^{-1}$) have the lowest. Alkynes and aromatics have intermediate MIR values. While this method cannot directly be used to determine ozone production in the concentrated engine plume (due to high NO_x mixing ratios) relative MIR values give a relative estimate of ozone production potential downwind.

For the direct exhaust samples, an average MIR value can be determined based on the hydrocarbon mixture:

$$\overline{\text{MIR}} = \frac{\sum \text{EI}_i \cdot \text{MIR}_i}{\sum \text{EI}_i}$$

Where EI_i and MIR_i are for the individual NMHCs measured in the exhaust. The average MIR value for the exhaust decreases with power due to a decrease in the proportion of alkenes (with high MIR values) and a relative increase in aromatics and alkanes. For the AE3007 engine, the average MIR value decreases from 5.9 $\text{gO}_3/\text{gVOC}^{-1}$ at 7% to 4.6 $\text{gO}_3/\text{gVOC}^{-1}$ at 30%, giving a decrease in ozone productivity of 22% (similar decreases were seen for the other engines; 7.4 to 5.8 $\text{gO}_3/\text{gVOC}^{-1}$ for the PW308 and 5.8 to 3.4 for the RB211 engine). Surprisingly, despite the low MIR value for CO it can produce a large amount of ozone due to its high EI in the exhaust. At 30% power, more ozone can be produced from CO oxidation than from oxidation of hydrocarbons (Fig. 8). Conversely at low power, production from alkenes dominates.

9. Discussion – HAPs emission

Additionally, aircraft exhaust includes a number of compounds the United States classifies as HAPs (EPA, 2008). These compounds are identified in Tables 2 and 3. In the plume samples, HAPs made up 27–42% of the measured emissions with formaldehyde dominating. The contribution of HAPs in the direct exhaust is lower (8–28% with an increase at higher power) because oxygenated species were not measured. Due to differences in measurement techniques and engine power settings, the direct and plume exhaust HAPs levels cannot be compared quantitatively. Further research is needed to determine the production and gas-particle partitioning of HAPs that can occur as the exhaust ages and cools.

10. Conclusions

The current research shows that the speciation of hydrocarbon emissions from aircraft is power dependent. Low engine powers (representative of idle conditions) produce a larger amount of total NMHCs composed primarily of alkenes and alkynes. As power increases, total emissions decrease and the speciation shifts towards the production of aromatics. The increasing importance of aromatics observed as power is increased is likely the result of a shift from cracking (forming predominantly alkenes) to growth of larger compounds (formation of aromatics). This shift causes a decrease in the reactivity of the emissions and therefore a decrease in the ozone formation potential.

At ground level, aircraft operated in the idle and taxi mode are the major source of emissions due to a combination of the higher emission indices and longer periods of time spent at these power conditions (even taking into account increased fuel flow rates at higher engine powers). These emissions also are the most likely to cause formation of ground level ozone. At altitude the shift in

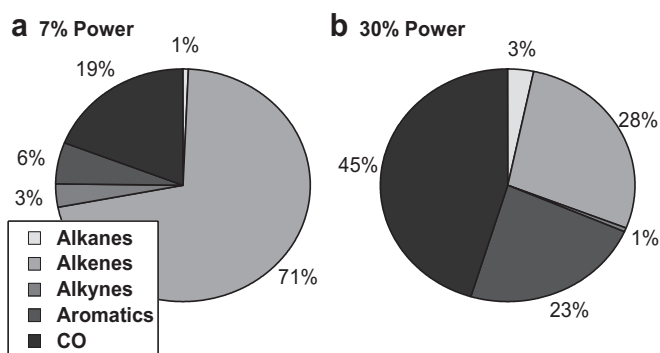


Fig. 8. Percentage of ozone formation potential for each hydrocarbon category for the AE3007 engine at 7% and 30% power.

speciation causes a larger relative emission of aromatics (some of which are HAPs). Because of the colder temperatures at cruise altitudes, these HAPs will have longer atmospheric lifetimes than those emitted at ground level.

Acknowledgements

This research was supported by the NASA Aeronautics Research Mission Directorate. Assistance during the field campaign was provided by Charles Hudgins (NASA Langley) and was facilitated by Southwest Airlines, Continental Airlines, FedEx and NASA Glenn Research Center. Analytical assistance was provided by Changlie Wey at NASA Glenn (CO₂ data) and Gloria Liu, Brent Love and Simone Meinardi at UC Irvine. John Kinsey at the EPA provided the APEX report and helpful suggestions during manuscript preparation. Assistance with manuscript preparation was also provided by Scott Herndon at Aerodyne Research, Inc. and Angela Baker at the Max Planck Institute for Chemistry.

References

- Anderson, B.E., Chen, G., Blake, D.R., 2006. Hydrocarbon emissions from a modern commercial airliner. *Atmospheric Environment* 40, 3601–3612.
- Apel, E.C., Calvert, J.G., Gilpin, T.M., Fehsenfeld, F., Lonneman, W.A., 2003. Non-methane hydrocarbon intercomparison experiment (NOMHICE): task 4, ambient air. *Journal of Geophysical Research* 108. <http://dx.doi.org/10.1029/2002JD002936>.
- Bauer, S.H., Jeffers, P.M., 1988. Mechanistic investigation of soot precursors. *Energy & Fuels* 2, 446–453.
- Carter, W.P.L., 1994. Development of ozone reactivity scales for volatile organic compounds. *Journal of the Air & Waste Management Association* 44, 881–899.
- Carter, W.P.L., 2010. Development of the SAPRC-07 chemical mechanism. *Atmospheric Environment* 44. <http://dx.doi.org/10.1016/j.atmosenv.2010.01.026>.
- Colman, J.J., Swanson, A.L., Meinardi, S., Sive, B.C., Blake, D.R., Rowland, F.S., 2001. Analysis of a wide range of volatile organic compounds in whole air samples collected during PEM-tropics A and B. *Journal of Analytical Chemistry* 73, 3723–3731.
- de la Rosa Blanco, E., Peck, J., Miake-Lye, R.C., Hills, F.B., Wood, E.C., Herndon, S.C., Annen, K.D., Yelvington, P.E., Leach, T., 2011. Minimizing sampling loss in trace gas emission measurements for aircraft engines by using a chemical quick-quench probe. *Journal of Engineering for Gas Turbines and Power* 133, 071602–071611.
- DuBois, D., Paynter, G.C., 2006. "Fuel Flow Method2" for Estimating Aircraft Emissions. SAE Technical Papers Series, 2006-01-1987.
- EPA, 1986. Research Protocol Method for Analysis of C₂ – C₁₂ Hydrocarbons in Ambient Air by Gas Chromatography with Cryogenic Concentration. Report No. ASRL-APCD-RPM 002. Environmental Protection Agency, Research Triangle Park, NC.
- EPA, 1999a. Compendium Method TO-15: Determination of Volatile Organic Compounds (VOCs) in Air Collected in Specially-Prepared Canisters and Analyzed by Gas Chromatography/Mass Spectrometry (GC/MS). Available online at: <http://www.epa.gov/ttn/amtic/files/ambient/airtox/to-15r.pdf> (accessed 15.04.10.).
- EPA, 1999b. Compendium Method TO-11A: Determination of Formaldehyde in Ambient Air Using Adsorbent Cartridge Followed by High Performance Liquid Chromatography (HPLC) [Active Sampling Methodology]. Available online at: <http://www.epa.gov/ttn/amtic/files/ambient/airtox/to-11ar.pdf> (accessed 15.04.10.).
- EPA, 2008. The Clean Air Act Amendments of 1990 List of Hazardous Air Pollutants. Available online at: <http://www.epa.gov/ttn/atw/orig189.html> (accessed 11.06.10.).
- FAA, 2010. FAA Aerospace Forecast Fiscal Years 2010–2030. Available online at: http://www.faa.gov/data_research/aviation/aerospace_forecasts/2010-2030/ (accessed 11.06.10.).
- Herndon, S.C., Rogers, T., Dunlea, E., Jayne, J., Miake-Lye, R., Knighton, B., 2006. Hydrocarbon emissions from in-use commercial aircraft during airport operations. *Environmental Science and Technology* 40, 4406–4413.
- Herndon, S.C., Wood, E., Northway, M.J., Miake-Lye, R., Thornhill, L., Beyersdorf, A., Anderson, B.E., Dowlin, R., Dodds, W., Knighton, W.B., 2009. Aircraft hydrocarbon emissions at Oakland international airport. *Environmental Science and Technology* 43, 1730–1736.
- Kinsey, J.S., Mitchell, W.A., Squier, W.C., Wong, A., Williams, C.D., Logan, R., Kariher, P.H., 2006. Development of a new mobile laboratory for characterization of the fine particulate emissions from heavy-duty diesel trucks. *Journal of Automobile Engineering* 220, 335–345.
- Kinsey, J.S., Hays, M.D., Dong, Y., Williams, D.C., Logan, R., 2011. Chemical characterization of the fine particle emissions from commercial aircraft engines during the aircraft particle emissions experiment (APEX) 1 to 3. *Environmental Science and Technology* 45. <http://dx.doi.org/10.1021/es103880d>.
- Kinsey, J.S., 2009. Characterization of Emissions from Commercial Aircraft Engines During the Aircraft Particle Emissions Experiment (APEX) 1 to 3. EPA-600/R-09/130. U. S. Environmental Protection Agency, National Risk Management Research Laboratory, Research Triangle Park, NC.
- Knighton, W.B., Rogers, T.M., Anderson, B.E., Herndon, S.C., Yelvington, P.E., Miake-Lye, R.C., 2007. Quantification of aircraft engine hydrocarbon emissions using proton transfer reaction mass spectrometry. *Journal of Propulsion and Power* 23, 949–958.
- McEnally, C.S., Pfefferle, L.D., 1997. Experimental assessment of naphthalene formation mechanisms in non-premixed flames. *Combustion Science and Technology* 128, 257–278.
- Schulz, H., Bandeira de Melo, G., Ousmanov, F., 1999. Volatile organic compounds and particulates as components of diesel engine exhaust gas. *Combustion and Flame* 118, 179–190.
- Schürmann, G., Schäfer, K., Jahn, C., Hoffmann, H., Bauerfeind, M., Fleuti, E., Rappenglück, B., 2007. The impact of NO_x, CO and VOC emissions on the air quality of Zurich airport. *Atmospheric Environment* 41, 103–118.
- Slemr, F., Giehl, H., Slemr, J., Busen, R., Schulte, P., Haschberger, P., 1998. In-flight measurement of aircraft non-methane hydrocarbon emission indices. *Geophysical Research Letters* 25, 321–324.
- Slemr, F., Giehl, H., Habram, M., Slemr, J., Schlager, H., Schulte, P., Haschberger, P., Lindermeier, E., Döpelheuer, A., Plohr, M., 2001. In-flight measurement of aircraft CO and nonmethane hydrocarbon emission indices. *Journal of Geophysical Research* 106, 7485–7494.
- Spicer, C.W., Holdren, M.W., Smith, D.L., Hughes, D.P., Smith, M.D., 1992. Chemical composition of exhaust from aircraft turbine engines. *Journal of Engineering for Gas Turbines and Power* 114, 111–115.
- Spicer, C.W., Holdren, M.W., Riggan, R.M., Lyon, T.F., 1994. Chemical composition and photochemical reactivity of exhaust from aircraft turbine engines. *Annales Geophysicae* 12, 944–955.
- Timko, M.T., Herndon, S.C., Wood, E.C., Onasch, T.B., Northway, M.J., Jayne, J.T., Canagaratna, M.R., Miake-Lye, R.C., Knighton, W.B., 2010a. Gas turbine engine emissions – part I: volatile organic compounds and nitrogen oxides. *Journal of Engineering for Gas Turbines and Power* 132. Article 061504.
- Timko, M.T., Onasch, T.B., Northway, M.J., Jayne, J.T., Canagaratna, M.R., Herndon, S.C., Wood, E.C., Miake-Lye, R.C., Knighton, W.B., 2010b. Gas turbine engine emissions – part II: chemical properties of particulate matter. *Journal of Engineering for Gas Turbines and Power* 132. Article 061505.
- Wang, H., Frenklach, M., 1994. Calculations of rate coefficients for the Chemically activated reactions of acetylene with vinylic and aromatic radicals. *Journal of Physical Chemistry* 98, 11465–11489.
- Warnatz, J., Mass, U., Dibble, R.W., 2006. *Combustion: Physical and Chemical Fundamentals, Modeling and Simulation, Experiments, Pollutant Formation*, fourth ed. Springer, New York City.
- Wey, C.C., Anderson, B.E., Hudgins, C., Wey, C., Li-Jones, X., Winstead, E., Thornhill, L.K., Lobo, P., Hagen, D., Whitefield, P., Yelvington, P.E., Herndon, S.C., Onasch, T.B., Miake-Lye, R.C., Wormhoudt, J., Knighton, W.B., Howard, R., Bryant, D., Corporan, E., Moses, C., Holve, D., Dodds, W., 2006. Aircraft Particle Emission Experiment, NASA/TM-2006-214382.
- Wong, H.-W., Yu, Z., Timko, M.T., Herndon, S.C., de la Rosa Blanco, E., Miake-Lye, R.C., 2011. Design parameters for an aircraft engine exit plane particle sampling system. *Journal of Engineering for Gas Turbines and Power* 133. <http://dx.doi.org/10.1115/1.4001979>.
- Wood, E.C., Herndon, S.C., Timko, M.T., Yelvington, P.E., Miake-Lye, R.C., 2008. Speciation and chemical evolution of nitrogen oxides in aircraft exhaust near airports. *Environmental Science and Technology* 42, 1884–1891.
- Yelvington, P.E., Herndon, S.C., Wormhoudt, J.C., Jayne, J.T., Miake-Lye, R.C., Knighton, W.B., Wey, C., 2007. Chemical speciation of hydrocarbon emissions from a commercial aircraft engine. *Journal of Propulsion and Power* 23, 912–918.